Wear Mechanism of Chromium Pre-Alloyed Sintered Steel

Róbert Bidulský[1,*], Marco Actis Grande[1], Jana Bidulská[2], Martin Vlado[2] and Tibor Kvačkaj[2]

[1] *Politecnico Torino-Alessandria Campus, Viale T. Michel 5, 15100 Alessandria, Italy*
[2] *Technical University of Košice, Faculty of Metallurgy, Letná 9, 04200 Košice, Slovakia*

(Received May 4, 2009; final form May 12, 2009)

ABSTRACT

The paper is focused on the wear mechanism of a chromium pre-alloyed Fe (Cr - Mo) - C sintered steel. The wear behaviour of the sintered steel is investigated through pin-on-disk tests. Two different processing conditions have been used, involving a slow cooling rate of 0.05 K/s and a process called sinter hardening with an average cooling rate of 6 K/s from the sintering temperatures (1453 and 1513 K). The microscopic investigations reveal deformed layers and tracks along the direction of sliding during wear. Particular attention has also been paid to the friction coefficient and to the role of porosity on wear.

Key words: pre-alloyed sintered steel, sinter hardening, sliding wear and microstructure

1. INTRODUCTION

Porous ferrous alloys, obtained via powder metallurgy (PM), are currently used in the production of structural parts, such as gears, cams and automotive valve seat applications, which undergo sliding, rolling or abrasive wear loading in service. To achieve the production of sintered parts with high-performance applications it is therefore necessary to apply a further optimization of the processing conditions.

Secondary operations are successfully used in the PM processing to achieve the desired wear and fatigue resistance as well improved material properties (strength and hardness) /1-5/. Coating, heat treating and steam treating are among the secondary operations that are successfully applied in the fabrication of finished PM parts /6/. Sinter hardening in vacuum furnaces has been shown to be an alternative to more traditional processing, offering cost savings and better part properties /7, 8/. The tempering operations, which can be carried out within the same sintering cycle, allow reducing internal stresses /9-11/ that influence mechanical properties as well as crack initiation and propagation.

Wear resistance (including mass loss and wear rates) of the investigated materials has been presented in previous work /12/; results suggested that the wear resistance using higher temperature and cooling rate (sinter hardening) was improved due to the shifting of ferrite - bainite to a dominant martensitic micro-structure.The microstructure characteristics represent an important parameter affecting the wear behaviour of sintered steels.

This work is focused on the role of the different sintering processes on the wear mechanisms of Fe (Cr - Mo) - C sintered steels and on the understanding of the wear mechanisms.

2. MATERIAL AND EXPERIMENTAL METHODS

Powder mixtures were homogenised in a Turbula mixer using Astaloy CrL powder (Höganäs AB), graphite powder and commercial AW wax powder as lubricant.

* Corresponding author: R. Bidulský,
Tel.:+39-0131-229232; fax:+39-0131-229399, E-mail: robert.bidulsky@polito.it

Specimens with a green density of ~7.0 g/cm^3 (=7.0 x 10^6 g/m^3) were obtained using a 2000 kN hydraulic press, in a disc-shaped mould (ϕ 40 mm) applying a pressure of 600 MPa. Sintering was carried out in the TAV vacuum furnace with argon back filling. Densities were evaluated using the water displacement method. The processing conditions are recorded in **Table 1**.

Table 1
Processing characterization of the sintered steel

Alloy No	Composition [in mass %]	Sintering conditions
A	Fe-1.5Cr-0.2Mo-0.65C	1453 K / SC* (0.05 K/s)
B	Fe-1.5Cr-0.2Mo-0.65C	1453 K / RC* (6 K/s)
C	Fe-1.5Cr-0.2Mo-0.65C	1513 K / RC* (6 K/s)

*SC-slow cooling rate, RC-rapid cooling rate

Wear test was carried out by means of pin-on-disc procedure. The disc was made of the investigated material. As a counter face, a WC-Co pin was used, having a rounded shape on top with ϕ 3 mm. The counter-pin was changed after the end of each test, in order to preserve the roundness of its top. All wear tests were performed in air and without any lubricant. The applied loads were 25 N. The rotation speed of the disc was 140 rpm. The distances of the pin position from the disc centre were 34 mm. The tested surface was polished with abrasive papers in order to determine a medium surface roughness equal (or less) to 0.8 μm, as specified in the ASTM G99–95a. Each test was interrupted after 300, 600, 900, 1200 and 2000 meters sliding distance and discs were weighed, using a precision scales with a sensitivity of 10^{-5} to determine the evolution of wear during each test.

The wear characterization of the chromium pre-alloyed sintered steels containing copper were carried out by means of optical microscopy, also determining the volume mass and the interconnected (open) porosity (according to UNI 7825), wear tracks features observations were carried out using SEM JEOL 7000F. Metallographic evaluations using a Leica Qwin image analysis system were carried out to evaluate pore shape and distribution.

3. EXPERIMENTAL RESULTS AND DISCUSSION

Table 2 reports the steady-state value of friction coefficient and **Fig. 1** show how the porosity content influence the steady-state value of friction coefficient.

Table 2
Porosity and the steady-state value of friction coefficient of the alloys

Alloy No	ρ_P*	ρ_S*	P_{Total}	Friction coefficient μ
	[g/cm^3]	[g/cm^3]	[%]	[-]
A	6.987	7.002	8.64	0.7397
B	6.983	6.973	9.01	0.7200
C	7.002	7.113	7.19	0.7578

* P-Pressing, *S-Sintering (g/cm^3 = 10^6 g/m^3)

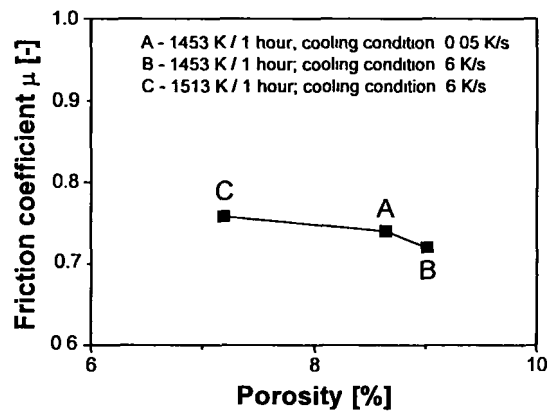

Fig. 1: Dependency of the steady-state value of friction coefficient on porosity

The results show that the steady-state value of friction coefficient decreases with the increasing amount of porosity. Using traditional PM methods, cold die

pressing and following sintering operations usually attain porosity value of 8-10% that are obtained in dependence on the sintered steel characteristics such as alloying additions and microstructure constituents. The friction properties are strongly dependent upon the sintered steel characteristics.

Figure 2 shows the trend of the friction coefficient as function of the sliding distance for the system A, sintered at 1453 K and slowly cooled.

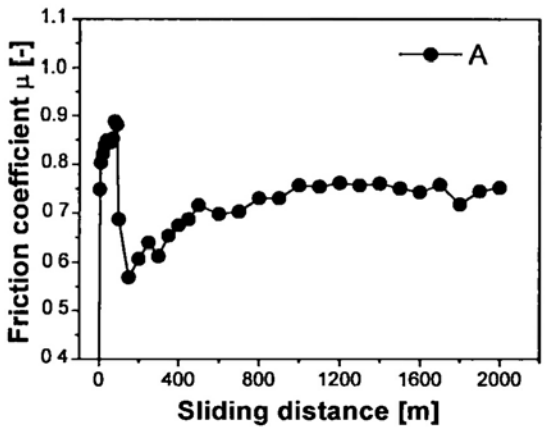

Fig. 2: Typical variation of friction coefficient (system A sintered at temperature of 1453 K and followed by slow cooling rate of 0.05 K/s)

The initial friction coefficient at the beginning of the test steeply rises to about 0.9 between the distance of 100 and 150 m. The next sliding showed reduction of the friction coefficient and reached the steady state. The steady state stage was observed after 800 m of sliding approximately.

Useful information on the wear mechanisms of the sintered steels was obtained by SEM analyses of the worn surfaces. The worn surfaces were characterized by the presence of fine grooves parallel to the sliding direction and flake-like fragments, typical of delamination wear, observed in the wear debris (**Figs. 3-5**).

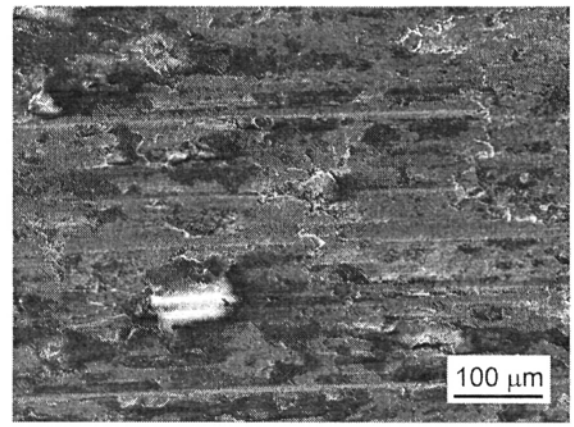

Fig. 3: The worn surfaces of the specimens A sintered at temperature of 1453 K and followed by slow cooling rate of 0.05 K/s

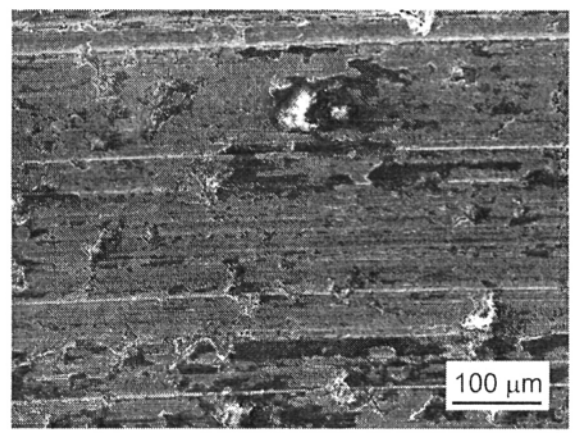

Fig. 4: The worn surfaces of the specimens B sintered at temperature of 1453 K and followed by rapid cooling rate of 6 K/s

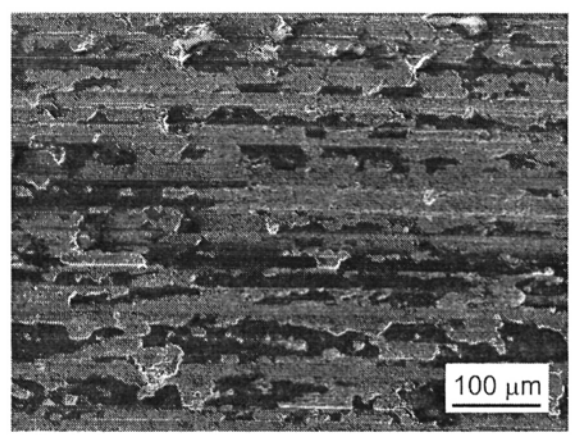

Fig. 5: The worn surfaces of the specimens C sintered at temperature of 1513 K and followed by rapid cooling rate of 6 K/s

The delamination wear mechanism postulates the consecutive steps /13/ of gross plastic deformation of the subsurface along the sliding direction, the subsequent nucleation of voids and cracks (in porous materials, the voids preexist in the form of pores; pores act as stress and strain concentrators, then the nucleation of cracks may be rather favored), the propagation of the cracks nearly parallel to the wear surface and the formation of wear sheets when cracks reach the surface. Therefore, plastic deformation took place on wear surfaces during wear tests. Contact pressure of wear surfaces increased with the increasing amount of porosity /14/.

The surface of chromium pre-alloyed powder is covered by a surface oxide layer consisting of mainly complex refractory oxides, inhomogeneous in thickness (**Fig. 6** and **Fig. 7**).

Karlsson *et al.* /15/ revealed that the above mentioned surface oxides are formed by a continuous iron oxide layer with a thickness of approximately 5.5-7 nm with the presence of some particulate compounds characterized by a high content of strong oxide forming elements such as Cr, Mn and Si. Hryha *et al.* /16/ observed within the dimples of inner-particle ductile fracture facets mainly complex refractory oxides with a dominant content of chromium oxide. It inhibits extensive intermetallic contact and adhesion between the sliding counterfaces of the wear system and leads to preferential shearing within the oxide.

The interpretation of the role of porosity on the wear resistance is not as simple as for the mechanical properties. The important parameters which specify the role of porosity are the amount of porosity and pore size. Dubrujeaud *et al.* /17/suggested that if the amount of porosity is higher than 10% and the pore size is bigger than 12 μm, the pores are filled with debris particles during wear. This enhances the wear resistance of the samples by increasing the real contact area and decreasing the contact pressure. The small wear debris can be trapped inside the open pores on the sliding surface, and this may lead to the main difference between the wear rate obtained from the depth loss and from the weight loss (**Figs. 8-10**).

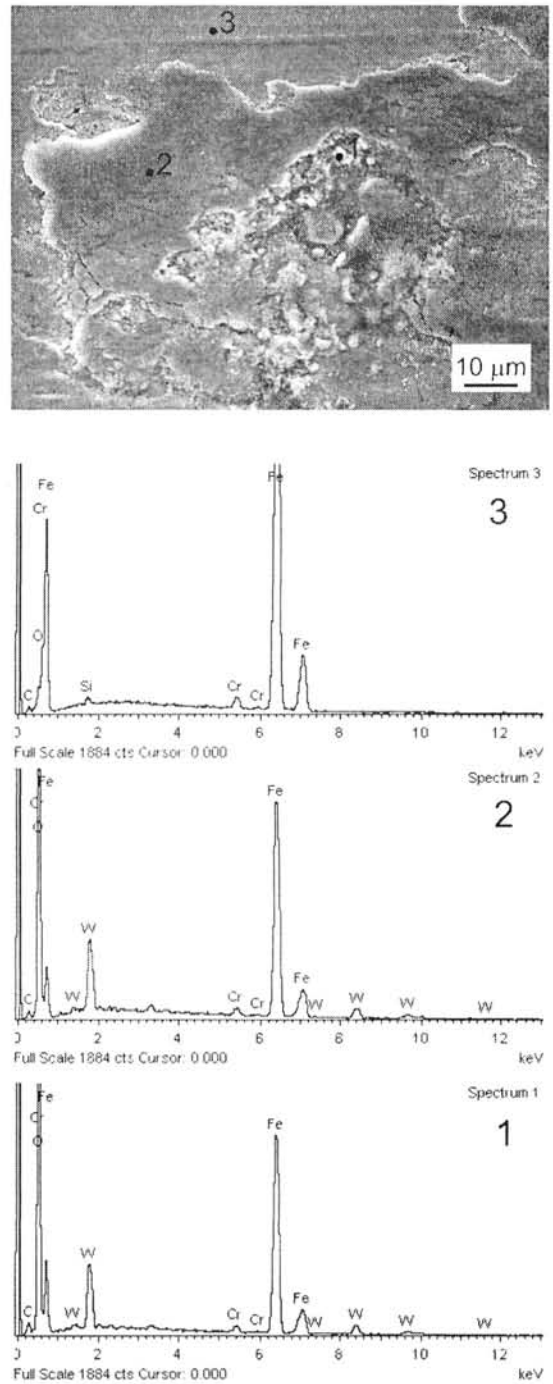

Fig. 6: A surface oxide layer on the worn surface of the specimens B sintered at temperature of 1453 K and followed by rapid cooling rate of 6 K/s

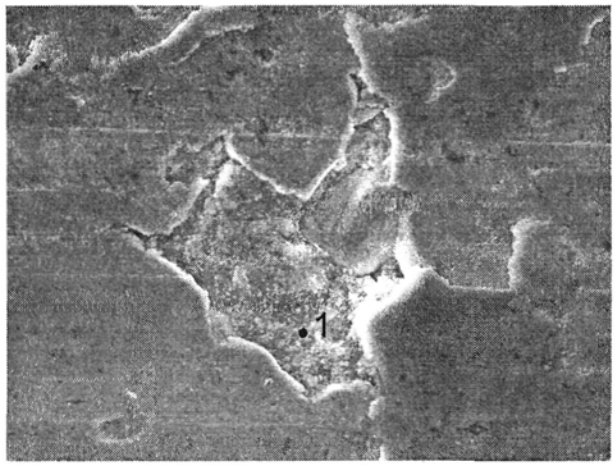

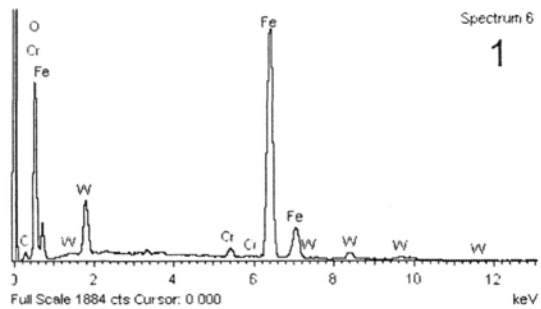

Fig. 7: A surface oxide layer on the worn surface of the specimens C sintered at temperature of 1513 K and followed by slow cooling rate of 6 K/s

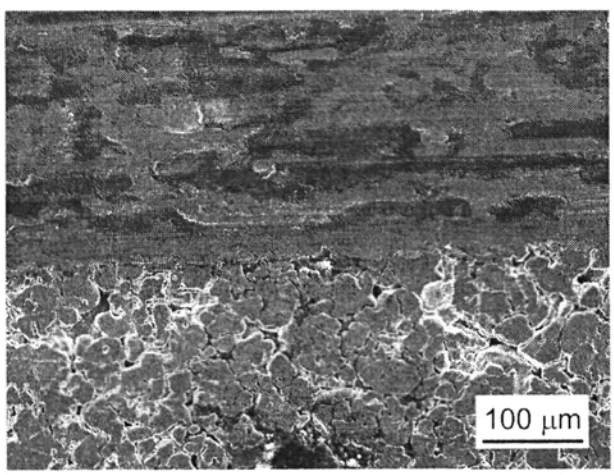

Fig. 8: The open pores on the sliding surface of the specimens A sintered at temperature of 1453 K and followed by slow cooling rate of 0.05 K/s

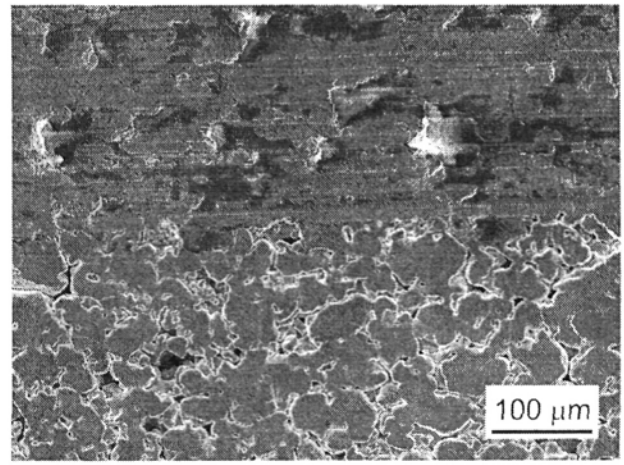

Fig. 9: The open pores on the sliding surface of the specimens B sintered at temperature of 1453 K and followed by rapid cooling rate of 6 K/s

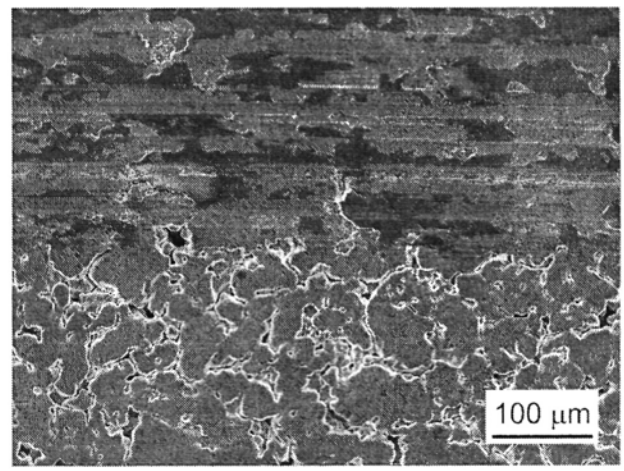

Fig. 10: The open pores on the sliding surface of the specimens C sintered at temperature of 1513 K and followed by rapid cooling rate of 6 K/s

However, the higher sintering temperature supported roundness and an overall reduction of pores, therefore promoting a significant increasing of wear resistance. Nevertheless, as shown from **Figs. 8-10** porosity is to be beneficial for enhancing the wear resistance by entrapping the wear debris and preventing the formation of large abrasive agglomerates, as it has been reported in /17/

4. CONCLUSION

This work is focused on the role of the different sintering processes on the wear mechanisms of chromium pre-alloyed Fe (Cr -Mo) - C sintered steel. The main conclusions are:

1. The results of friction coefficient shows that the steady-state value of friction coefficient decreases with the increasing amount of porosity.
2. The microscopic investigation reveals that delamination and oxidation wear are the main wear mechanisms in wear tests.
3. Pores play an important role representing the potential sites of the first microcracks forming and positively influencing the wear process by entrapping the wear debris and preventing the formation of large abrasive agglomerates.

ACKNOWLEDGEMENTS

R. Bidulský thanks the Politecnico di Torino and the Regione Piemonte for co-funding by the fellowship.

REFERENCES:

1. G. Straffelini, T. Marcu Puscas and A. Molinari: *Metall. Mater. Trans. A*, **31**, No. 12, 3091-3099 (2000).
2. R. Bidulský and M. Actis Grande: *Key Eng. Mater.*, **409**, 390-393 (2009).
3. R. Bidulský, M. Actis Grande, J. Bidulská and T. Kvačkaj: *Mater. Tehnol.*, **43**, No. 6, 303-307 (2009).
4. D. Grimanelis and T.S. Eyre: *Wear*, **262**, No. 1-2, 93-103 (2007).
5. R. Bidulský, M. Actis Grande, M. Kabátová and J. Bidulská: J. Mater. Sci. Technol., 25, No. 5, 607-610 (2009).
6. G.F. Bocchini: *Adv. Powder Metall. Part. Mater.*, **4**, 77-106 (1992).
7. R. Bidulský, M. Actis Grande and M. Kabátová: *Powder Metal. Prog.*, **8**, No. 4, 196-199 (2008).
8. L.A. Dobrzański, Z. Brytan, M. Actis Grande, M. Rosso and E.J. Pallavicini: *J. Mater. Process. Tech.*, **162-163**, 286-292 (2005).
9. L. Ceniga: *Acta Mech. Sinica*, **24**, No. 2, 189-206 (2008).
10. L. Ceniga: *J. Therm. Stresses*, **31**, No. 8, 728-758 (2008).
11. L. Ceniga: *J. Therm. Stresses*, **31**, No. 9, 862-891 (2008).
12. R. Bidulský and M. Actis Grande: *High Temp. Mater. Process.*, **27**, No. 4, 249-256 (2008).
13. D. Grimanelis and T.S. Eyre: *Surf. Coat. Technol.*, **201**, No. 6, 3260-3268 (2006)
14. H. O. Gulsoy, M. K. Bilici, Y. Bozkurt and S.Salman: *Mater. Des.*, **28**, No. 7, 2255-2259 (2007)
15. H. Karlsson, L. Nyborg and S. Berg: *Powder Metall.*, **48**, No. 1, 51-58 (2005).
16. E. Hryha, L. Čajková and E. Dudrová: *Powder Metall. Prog.*, **7**; No. 4, 181-197 (2007).
17. B. Dubrujeaud, M. Vardavoulias and M. Jeandin: *Wear*, **174**, No. 1-2, 155-161 (1994).